

NAR Breakthrough Article

Proteomic identification of histone post-translational modifications and proteins enriched at a DNA double-strand break

Pingping Wang^{1,2}, Stephanie Byrum³, Faith C. Fowler¹, Sangita Pal^{1,2}, Alan J. Tackett³ and Jessica K. Tyler^{1,*}

¹Weill Cornell Medicine, Department of Pathology and Laboratory Medicine, New York, NY 10065, USA, ²Genes and Development Graduate Program of the University of Texas MD Anderson Cancer Center, UT Health Graduate School of Biomedical Sciences, Houston, TX 77030, USA and ³University of Arkansas for Medical Sciences, Department of Biochemistry and Molecular Biology, Little Rock, AR 72205, USA

Received April 25, 2017; Revised August 29, 2017; Editorial Decision August 31, 2017; Accepted September 13, 2017

ABSTRACT

Here, we use ChAP-MS (chromatin affinity purification with mass spectrometry), for the affinity purification of a sequence-specific single-copy endogenous chromosomal locus containing a DNA double-strand break (DSB). We found multiple new histone post-translational modifications enriched on chromatin bearing a DSB from budding yeast. One of these, methylation of histone H3 on lysine 125, has not previously been reported. Among over 100 novel proteins enriched at a DSB were the phosphatase Sit4, the RNA pol II degradation factor Def1, the mRNA export protein Yra1 and the HECT E3 ligase Tom1. Each of these proteins was required for resistance to radiomimetics, and many were required for resistance to heat, which we show here to cause a defect in DSB repair in yeast. Yra1 and Def1 were required for DSB repair *per se*, while Sit4 was required for rapid inactivation of the DNA damage checkpoint after DSB repair. Thus, our unbiased proteomics approach has led to the unexpected discovery of novel roles for these and other proteins in the DNA damage response.

INTRODUCTION

Our genomes frequently encounter many different types of DNA lesions. However, DNA double-strand breaks (DSBs) are arguably the most deleterious, since they can cause chromosome rearrangements when misrepaired and loss of

chromosome arms or cell death if unrepaired (1). Both endogenous factors, such as DNA replication and reactive oxygen species, and exogenous factors, such as chemotherapeutics, can give rise to DSBs. In order to maintain genomic integrity, it is essential to accurately repair DSBs. The key importance of DSB repair is highlighted by the fact that its deregulation is at the heart of tumorigenesis and many other human disease syndromes (2).

In order to repair DSBs, cells have developed an elaborate DNA damage response. The DNA damage response is a complex network of cellular pathways that sense, signal and repair DSBs (3). It is initiated by surveillance proteins, which monitor DNA integrity and activate the DNA damage cell cycle checkpoint in order to avoid the transmission of damaged genetic information to the progeny cells. The DNA damage response also involves recruitment, to the DNA lesion, of the proteins that mediate the repair of the DNA molecule, followed by the subsequent inactivation of the DNA damage cell cycle checkpoint.

Repair of DSBs is mediated by several different repair pathways, the two most prominent being homologous recombination (HR) and non-homologous end joining (NHEJ) (1). NHEJ is referred to as 'non-homologous' because the DNA break ends are directly ligated without the need for a homologous template, in contrast to homology directed repair, which requires a homologous sequence to guide repair. In mammalian cells, NHEJ is mainly used in G₁ phase of the cell cycle, while HR is used during S and G₂ phases when the sister chromatid is available to provide the sequence homology (4). By contrast, mammalian embryonic stem cells predominantly repair DSBs via HR (5). Although the use of the homologous template enables

*To whom correspondence should be addressed. Tel: +1 746 4357 212; Email: jet2021@med.cornell.edu

cells to accurately repair DSBs by HR, this repair process is a great deal more complex than NHEJ. An early step in HR is the resection of the 5' ends of the DNA break, creating 3' overhangs that become bound by the single-stranded binding protein RPA. The Rad51 protein replaces RPA to form a nucleofilament on the single-stranded DNA, and this occurs with the aid of the recombinase Rad52 (6) and the DNA translocase Rad54 (7). This nucleofilament searches for DNA sequences with homology to the 3' overhang. Once found, the nucleofilament invades the identical donor DNA by strand invasion and DNA synthesis extends the end of the invading 3' strands to restore the DNA sequence (1). Intriguingly, the many stages of HR have to occur in the chromosomal context of the genome within chromatin where the DNA is wrapped around the core histone proteins H3, H4, H2A, and H2B (8). While we know that multiple histone PTMs are involved in the DNA damage response to DSBs (9), our knowledge of the machinery that modifies and alters the chromatin to enable HR is far from complete.

Given the complexity of the DNA damage response, we postulated that novel proteins that contribute to DSB repair remain to be discovered. A great deal of our knowledge of the mechanism of HR has come from studying the DSB within the *MAT* locus induced by the sequence-specific homothallic (HO) switching endonuclease in *Saccharomyces cerevisiae* (10). The HO lesion is repaired by homologous recombination using homology at the hidden *MAT* right (*HMR*) or hidden *MAT* left (*HML*) locus, resulting in mating type switching (11). Accordingly, we isolated chromatin fragments adjacent to the endogenous single-copy *MAT* locus containing the HO lesion, based on our previously developed chromatin affinity purification with mass spectrometry (ChAP-MS) method (12). Proof of concept of the ChAP-MS method has been provided previously by its ability to detect enrichment of proteins at the single copy chromosomal yeast *GALI* gene that were known to be involved in its transcriptional activation (13). Using this unbiased method, we identified new histone PTMs occurring at DSBs and uncovered novel unexpected roles for multiple proteins in the DNA damage response.

MATERIALS AND METHODS

Plasmid construction

Plasmid *pFA6a-2LEXA-His3MX6* was constructed by inserting DNA oligonucleotides containing two tandem copies of *LEXA* DNA binding site (*2LEXA*) into the *pFA6a-His3MX6* plasmid (14) *Bgl*II site, which was concomitantly disrupted upon ligation. The DNA oligonucleotides containing *2LEXA* (*2LEXA.delBglII-F*: GATCGCGCTACTGTATATATATACAGTAGCGCC TACTGTATATATATACATA

CGCG and *2LEXA.delBglII-R*: GATCCGCGTACT GTATATATATACAGTAGGGC

GCTACTGTATATATATACAGTAGCGC) were phosphorylated and annealed, before being ligated with *pFA6a-His3MX6* vector that had been *Bgl*II digested and dephosphorylated. The ligation product was transformed into chemically competent *E. coli* cells, and *Bgl*II negative clones

were selected for sequencing to screen for *2LEXA* correctly inserted into the *pFA6a-2LEXA-His3MX6* plasmid.

Yeast strain construction

The yeast strains used in this study are all listed in Supplemental Table S6. To make yeast strain PWY001 that has *2LEXA* sites integrated about 500 bp to the right of the HO cut site at the *MAT* locus on Chr III, DNA fragments spanning the *2LEXA* and *His3MX* cassette were PCR amplified from the plasmid *pFA6a-2LEXA-His3MX6* using primers HOcs-*2LEXA-HIS-F*: ACCTTCGGCTTCACAATT

TGTTTTTCCACTTTTCTAACAGCGGATCCCCGG GTTAATTAA, and HOcs-*2LEXA-HIS-R*: GGCGAATAAGATAAAGATAAGTTTGAAAGGTGA TAAACGAAT

TCGAGCTCGTTTAAAC. These primers include homology 500 bp distal to the HO cut site at the *MAT* locus on Chr III, and then transformed into strain JRY2334. Transformants were selected on synthetic minus histidine plates, and screened for clones with positive *2LEXA* insertion at the target region as determined by PCR screening. Plasmid *pLexA-PrA-Trp* expressing the LexA-Protein A fusion protein (13) was transformed into strain PWY001 to make strain PWY011. Strain PWY002 with the galactose-inducible *HO* gene integrated at the *ADE3* locus was constructed by transforming the linearized plasmid *pYI-Pade3HO* (kindly provided by Dr Virginia Zakian) into PWY001, following the procedures described in (15). The yeast strain PWY81 containing the HO cut site (HOcs) at the genomic *ADH1* gene was constructed by transforming into strain JCY004 with DNA fragments PCR amplified from the HOcs-13Myc-KanMX cassette at the 3' end of the *ADH1* gene using genomic DNA extracted from strain PCY23 (a kind gift from Dr Sukesh R. Bhaumik) as PCR template (16). The positive transformants were selected on G418 plates, and screened for clones that contain HOcs inserted at the 3' end of the *ADH1* gene.

Western blot analysis of Rad53

For the transient zeocin time course experiments, cells were grown to mid-log phase, and treated with zeocin (10 mg/ml stock solution in H₂O) at a final concentration of 15 µg/ml (or 30 µg/ml for Supplementary Figure S3C) for 30 min. Cells were then washed three times in fresh YPD medium to remove zeocin, and harvested at the indicated time points by centrifugation. Yeast whole cell extracts were prepared using the TCA method as has been described before (17) and separated on 7.5% SDS-PAGE gels. Anti-Rad53 antibody (EL7 clone (18)) was used to detect Rad53 protein. Anti-G6PDH (Sigma) was used as a loading control.

PCR analysis of HO cutting repair efficiency

For each time point, yeast cells were collected by centrifugation and genomic DNA was extracted. A multiplex PCR assay was performed as previously described (19) using *HOMAT* and *RAD27* (as a control) primers. PCR products were separated by 1.5% agarose gel electrophoresis, stained by SYBR safe dye and visualized by ProteinSimple Imager

(FluorChem E system). The *RAD27* products are expected to be ~1.4 kb, while *HOMAT* primers are expected to amplify *MAT α* products ~1.1 kb, and *MAT α* ~1.2 kb. Quantifications for the relative amount of *MAT α* or *MAT α* during HO cutting and repair was performed using AlphaView software on a ProteinSimple gel documentation machine.

Serial dilution assay

Yeast cells were grown in the appropriate media until they reached mid-log phase. Cells were collected by centrifugation, and resuspended in sterile Millipore H₂O. Cells were 10-fold diluted in sterile H₂O and cell suspensions were transferred onto the appropriate agar plates by a sterile spotter with 6 × 8 pins. Yeast plates were incubated in 30°C for 3 days before being photographed. For yeast drug sensitivity tests, cells were grown in YPD media, and spotted onto YPD agar plates supplemented with the indicated amount of drug. For yeast HO sensitivity tests, yeast strains with *GALHO* integrated at the *ade3* locus were grown in YPD to mid-log phase before being washed with YEP to remove glucose. Cells were resuspended in YEP + 2% raffinose and allowed to grow at least 6 h before being subjected to serial dilution assays. The ‘glucose’ and ‘galactose’ plates are YPD and YEP + 2% raffinose + 2% galactose, respectively. As for yeast strains with pGALHO (*URA3*) plasmids, cells were grown up in SC-ura + 2% glucose media. Mid-log phase cells were washed three times to remove glucose, and resuspended in SC-ura + 2% raffinose and allowed to grow at least 6 hr before being subjected to serial dilution assays. The ‘glucose’ and ‘galactose’ plates in Figure 5A are SC-ura + 2% glucose and SC-ura + 2% raffinose + 2% galactose, respectively.

RNA extraction and quantitative RT-PCR

Yeast RNA was extracted using the MasterPure™ Yeast RNA Purification Kit (Epicentre) following the manufacturer’s protocol. cDNA was synthesized using Transcriptor First Strand cDNA Synthesis Kit (Roche). Before reverse transcriptase was added to the reaction, a mixture of RNA and the anchored-oligo(dT)18 primer was denatured by heating at 65°C for 10 min and then cooled on ice. The cDNA synthesis reaction was performed at 55°C for 30 min, and then placed at 85°C for 5 min to inactivate the reverse transcriptase. A reaction without the reverse transcriptase was performed as a negative control. Quantitative PCR was then performed using LightCycler 480 SYBR Green 1 Master (Roche) on a LightCycler 480 instrument. The *YRA1* transcript level was normalized to *ACT1*, which was a control transcript.

SILAC-chromatin affinity purification and mass spectrometry

Yeast strains were grown at 30°C in synthetic medium lacking tryptophan, supplemented with either isotopically heavy lysine (¹³C₆) for control strains that are lacking *GALHO* in the genome, or isotopically light lysine (¹²C₆) for DSB-inducible strains at 70 mg/l. Cells were grown in media supplemented with 2% glucose until they reached

mid-log phase, and then washed with media without glucose before being resuspended in media containing 2% raffinose. Cells were allowed to grow 12 h in raffinose media to reach 0.5 OD₆₀₀/ml, before 2% galactose was added to induce HO expression. Two hours after galactose induction, cells were cross-linked with formaldehyde at 1.25% final concentration for 5 min, and quenched with 0.125 M glycine for 5 min at room temperature. Afterwards, cells were collected by centrifugation and washed once with cold Millipore H₂O. Cells were resuspended in suspension buffer (20 mM HEPES pH 7.4, 1.2% polyvinylpyrrolidone) at 100 μl/g of cell pellet, and then frozen in liquid nitrogen in a drop-wise manner. The frozen cells were stored at –80°C before being further processed. For each ChAP analysis, 6 L of control and 6 L of experimental cultures were prepared, respectively. Chromatin affinity purification using IgG beads and subsequent mass spectrometry analysis was performed following the procedures described previously (20). Briefly, the proteins were identified by Mascot with the following parameters: precursor ion tolerance of 10 ppm, fragment ion tolerance of 0.65 Da, false discovery rate of 1%, database search using the UniProtKB restricted to *Saccharomyces cerevisiae* (7802 entries), Lys6 heavy label, fixed modification of carbamidomethyl (C), variable modifications of oxidation (M), acetyl (protein N-term), mono-, di-, tri-methylation (K), acetylation (K), phosphorylation (ST) and ubiquitination (K). Intensities for each identified peptide were manually extracted and the percent light ratio was calculated as $L_{avg}/(L_{avg} + H_{avg})$. The ribosomal threshold for ChAP 1, ChAP 2, ChAP 3 and ChAP4 was 53.86% + 4.23% (1 standard deviations), 56.15% + 2.67% (1 SD), 46.38% + 1.54% (1 SD) and 50.74% + 1.86% (1 SD), respectively (Supplemental Table S1). The mass spec data are shown in Supplemental Tables S4 and S5. We also identified the ratio of heavy to light peptides and the total intensities of light plus heavy peptides for each protein using the same settings in MaxQuant for each ChAP experiment. The ratios were transformed to log₂ and scaled to have a mean of 0 and standard deviation of 1. The total intensities were transformed to log₁₀. The log₂ normalized ratios are plotted against the log₁₀ total intensity values in order to view the distribution of the mass spectrometric data. Each protein is also colored based on the percent light calculation (Supplementary Figure S2).

Pulsed field gel electrophoresis (PFGE)

Mid-log phase yeast cells were treated with zeocin (final concentration at 60 μg/ml for *sit4Δ* (from BY4741 deletion library) or *YRA1 DAmP* (from the DAmP library), or 45 μg/ml for *def1Δ* (JSY568)) for 90 min before being washed and then released into fresh YPD media. Cells that had been harvested at the indicated time points, were subjected to genomic DNA preparation and embedded in an agarose plug, as described in the manual for the CHEF Genomics DNA plug kit (Bio-Rad, 170-3593). The plugs and the yeast chromosome DNA size standard were loaded into the wells of a 1% agarose gel, which was soaked in 0.5 × TBE buffer for electrophoresis at 14°C for 24 h in a Bio-Rad CHEF-DR III System coupled to a cooling module. The setting was initial switch time 60 s, final switch time 120 s, ran at 6

volts/cm, and at a 120° angle. The agarose gels were stained with SYBR safe and visualized with a ProteinSimple Imager (FluorChem E system).

RESULTS

Identification of proteins and PTMs enriched at a single-copy site-specific chromosomal DSB

In order to identify novel proteins and PTMs that may be involved in the DNA damage response during HR, we took advantage of the HO endonuclease-induced DSB at the *MAT* locus in budding yeast *S. cerevisiae* (hereafter shortened to yeast) (Figure 1A). Fusion of the *HO* gene to the *GALI* promoter (*pGALI*) enables temporal control of DSB induction upon addition of galactose (21) (Figure 1B). To allow affinity purification of chromatin fragments from the endogenous *MAT* locus bearing the HO lesion, we integrated two *LEXA* DNA binding sites adjacent to the *MAT* HO site and constitutively expressed the LexA DNA binding domain fused to Protein A (LexA-PrA) (Figure 1B). The *LEXA* DNA binding sites were inserted ~500 bp to the right of the HO site, in order to avoid the loss of the double-stranded LexA DNA binding site and therefore loss of LexA-PrA binding which would occur upon DNA resection if the *LEXA* sites were closer to the HO lesion. While resection on a small subset of the templates can extend beyond 2 kb (22), we chose 500 bp from the HO site for the *LEXA* binding sites as a compromise between being able to detect proteins recruited to the vicinity of a DSB while still maintaining mostly dsDNA templates for *LEXA* binding. Locating the *LEXA* binding sites further away from the HO site would have reduced detection of proteins enriched at the DSB due to our average shearing size of 500–1000 bp. We acknowledge that this technique will not select for proteins enriched as binding to ssDNA during DSB repair and are developing different technologies for that purpose. Furthermore, while histones are known to be removed from around the DSB, we do not expect histones to be depleted from the dsDNA, because the kinetics of histone removal is not temporally separable from DNA resection and chromatin reassembly is coupled to DNA repair (23). Using semi-quantitative multiplex PCR with the primers indicated in Figure 1A to amplify over the HO site, an intact *MAT α* locus yields a 1.1 kb PCR product, while repair using the homologous sequences from *HML α* yields a 1.2 kb PCR product from the *MAT α* locus (Figure 1C). The control PCR product is generated from another chromosome and serves for normalization, where reduction of the total relative *MAT* PCR product level below 100% reflects the presence of a DSB at the *MAT* locus (Figure 1C and D). Using this assay, the HO-induced DSB generation and repair was very efficient (Figure 1C and D). The HO lesion was observed in ~80% of the cells 2 h after galactose-mediated induction of the HO endonuclease. Glucose was added 2 h after galactose addition to repress transcription of the HO gene to enable repair, and repair of ~90% of the *MAT* loci was apparent at 7 h (Figure 1D).

From the analysis above, we selected the maximal time of DSB induction (2 h after galactose addition) for the ChAP-MS procedure. To measure enrichment of proteins and PTMs in the vicinity of the HO-induced DSB site, we

used stable isotope labeling of amino acids in cell culture (SILAC)-based mass spectrometry (13). Specificity of enrichment at the DSB was determined by purifying the same chromatin fragment from an isogenic yeast strain lacking the gene encoding HO endonuclease. In brief, we grew two yeast cultures: the culture with the inducible DSB undergoing repair (+HO) was labeled with light lysine ($^{12}\text{C}_6$), and the culture with no HO endonuclease (–HO) was labeled with heavy lysine ($^{13}\text{C}_6$) (Figure 1E). After formaldehyde cross-linking, the two populations of cells were mixed in a 1:1 ratio by weight. The chromatin was then sheared to ~0.5–1 kb fragments, and we affinity purified the LexA-PrA-bound chromatin fragments using IgG beads (Supplementary Figure S1) (13). The percentage of light lysine for each identified protein was determined by mass spectrometric analysis. An unspecific binding threshold was established based on the averaged percentage of light isotope of the ribosomal proteins that were considered to be contamination proteins during the purification (Supplemental Table S1). Proteins or histone PTMs enriched in the vicinity of a DSB are expected to have a percentage of light lysine one standard deviation above the unspecific threshold (Figure 1E, Supplemental Table S1, Figure S2). We performed ChAP-MS from cells that were wild type (WT) for DNA repair on two independent occasions, including more cells the second time (Figure 1F). The most prominent cellular protein in all ChAP samples was LexA-PrA, indicating the specificity of the procedure (Supplementary Figure S1). In order to increase the proportion of cells that had the HO lesion at the time of the ChAP procedure, we also performed ChAP from strains that were deleted for the genes encoding the Rad52 and Rad54 homologous recombinational repair proteins (Figure 1F).

Proteomic identification of histone PTMs enriched at a DSB site

Mass spectrometry of our four ChAP samples identified many histone PTMs with a high degree of enrichment at the DSB (Table 1). These included histone PTMs that were previously shown to be enriched upon DNA damage and/or functionally important for the DNA damage response (Table 1, Group 1), such as H3 K14, K18, K23 and K27 acetylation and H4 K5, K8, K12 and K16 acetylation (19), H3 K56 acetylation (24,25), and H2B lysine 123 ubiquitination (26). In addition to histone PTMs known to be involved in the DNA damage response, we also identified histone PTMs enriched in the vicinity of the DSB that have not previously been implicated in DSB repair (Table 1, Group 2). These included H2A K4ac K7ac, H2B K6ac K11ac, H2B K16ac, K17ac and H3 K122ac K125me. Given that these histone PTMs were enriched at DSBs with very high ratios of light lysine and given our success in identifying histone PTMs known to be involved in the DNA damage response (Table 1), we predict that these novel histone PTMs enriched at the DSB will also play roles during DSB repair. Noteworthy, H3 K125me has not been reported previously in yeast, to our knowledge, representing a new histone PTM.

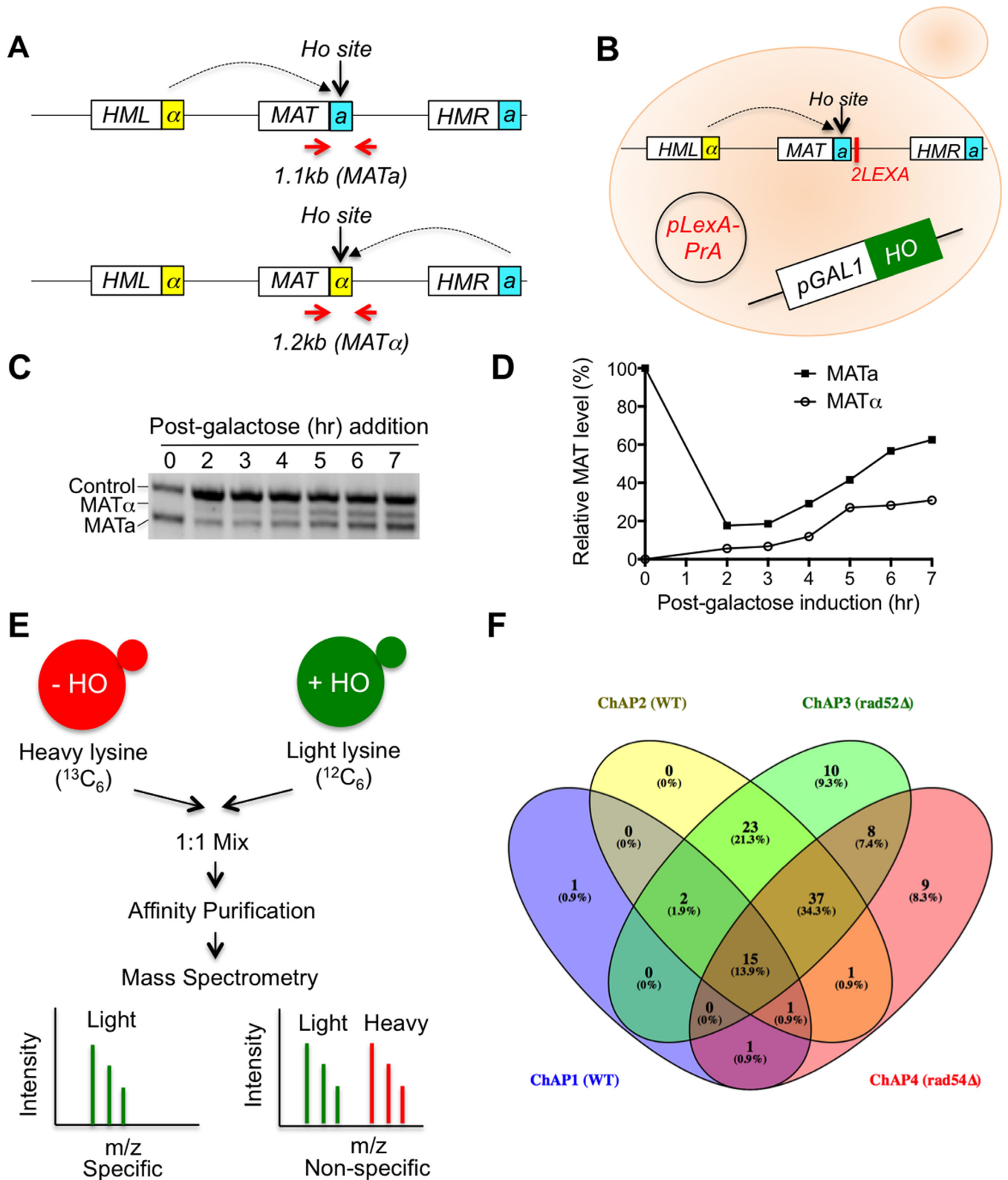


Figure 1. Using the ChAP-MS method to identify new proteins and histone PTMs at DSBs. (A) Schematic of the yeast mating type loci. The primers used for the PCR analysis for the dynamics of HO cutting/repair are shown in red and the respective product sizes are indicated. (B) Schematic of the key elements in the yeast strains used for ChAP-MS, as explained in the text. (C) Analysis of cutting and repair in strain PWY012, using the primers shown in A. Galactose was added at time 0 and glucose at 2 hr. The control was a *RAD27* gene product on a different chromosome. (D) Quantification of C, with *MAT* PCR products normalized to the control. (E) Schematic of SILAC based proteomic strategy for purifying proteins that specifically bind near the DSB, as described in the text. The strain lacking *pGAL1HO* (PWY011) is indicated by the red yeast cell ‘-HO’ while the green yeast cell ‘+HO’ represents the isogenic yeast strain (PWY012) with *pGAL1HO*. (F) Venn diagram of the common proteins found to be enriched at the DSB for each ChAP-MS analysis, made using the Venny^{2.1} software.

Table 1. List of histone PTMs identified as enriched at the HO-induced DSB site

Group #	Histone	PTM	ChAP1 (WT)	ChAP2 (WT)	ChAP3 (<i>rad52Δ</i>)	ChAP4 (<i>rad54Δ</i>)
Group 1	H3	K14ac	89.10%	55.60%	20.55%	86.28%
	H3	K18ac K23ac	57.70%	100.00%	88.87%	78.60%
	H3	K27ac	N.I	96.00%	N.I	95.70%
	H3	K56ac	N.I	60.20%	N.I	50.12%
	H4	K5ac K8ac	N.I	88.50%	N.I	N.I
	H4	K12ac k16ac	97.70%	100.00%	82.83%	92.27%
	H2B	K123ub	N.I	68.60%	N.I	42.19%
	H2A	K4ac K7ac	N.I	67.70%	N.I	45.45%
Group 2	H2B	K6ac K11ac	99.50%	N.I	N.I	N.I
	H2B	K16ac	100.00%	99.40%	82.47%	N.I
	H2B	K17ac	N.I	99.70%	N.I	N.I
	H3	K122ac K125me	95.80%	N.I	N.I	N.I

The percentage of light lysine for a given histone PTM is shown (%)

Group 1 include histone PTMs known to be involved in DSB response or repair;

Group 2 include new histone PTMs identified as enriched at the HO-induced DSB site by proteomic analyses.

N.I indicates not Identified.

Identification of novel DNA damage response proteins

We identified numerous proteins enriched at the HO lesion in our ChAP-MS analyses that were already known to function at DSB breaks (Supplemental Table S2). Importantly, we did not find any known repair proteins to be depleted from the HO lesion in our ChAP-MS analyses, providing validation of our approach. In addition to the known DSB response proteins, we found 108 additional proteins enriched in the vicinity of the DSB that do not have clear roles in the DNA damage response to DSBs (Supplemental Table S3). Eighty one of these 108 proteins were enriched at the DSB in WT cells (Figure 1F). Most of these proteins (77/81) were also enriched at the DSB in *rad52Δ* cells while an additional 18 proteins were enriched at the DSB in *rad52Δ* cells but not in WT cells. 55/81 proteins that were enriched at the DSB in WT cells were also enriched at the DSB in *rad54Δ* cells, while an additional 17 proteins were enriched at the DSB in *rad54Δ* cells but not in WT cells. Meanwhile 8 proteins were enriched at the DSB in both *rad52Δ* and *rad54Δ* cells, but not in WT cells (Supplemental Table S3, Figure 1F). The proteins that were specifically enriched or depleted from the WT, *rad52Δ* or *rad54Δ* cells likely reflect their being recruited to the DSB at specific times in DSB repair. Each ChAP analysis identified 700–1200 total proteins as enriched, depleted or not changed at the DSB (Supplemental Tables S4 and S5), indicating that the analyses were not saturating. The fact that the analyses are not saturating is likely to be a major reason for the variability between the two repeats of the experiment in wild type cells. In addition, the total number of cells used in the second repeat was twice as much as that used in the first. Furthermore, we typically find variability in the exact timing of HO induction and subsequent repair, as well as the degree of synchrony in the cell populations, between independent experiments. Regardless, we identified numerous new proteins enriched at a DSB.

From our analyses, we selected 27 non-essential and 28 essential proteins for further characterization of their role in the DNA damage response. We focused on what we considered to be the most interesting proteins enriched in the vicinity of a DSB in at least one ChAP analysis that had a nuclear localization and that had not clearly been implicated previously in DSB repair. First, we determined if the

proteins enriched at DSBs were functionally important for the DNA damage response by measuring the contribution of the candidate genes to resistance to DSBs by serial dilution analysis on plates with and without the radiomimetic zeocin. We used isogenic yeast strains deleted for the non-essential candidate genes, or with hypomorphic DAmP (Decreased Abundance by mRNA Perturbation (27)) alleles of essential genes. DAmP alleles have a Kanamycin resistance cassette inserted into the 3' UTR of the essential gene of interest, leading to reduced stability of the mRNA transcript. As a result, the level of essential proteins are decreased by DAmP alleles. Deletion of the non-essential candidate gene *CBF1*, *DEF1*, *NPL3*, *TOM1*, *PAT1*, *SIT4*, *GAS1*, *NPT1* or *PPZ1*, or DAmP alleles of essential gene *SIS1*, *ACS2*, *YRA1*, *GUK1*, *PMI40* or *ERG13* conferred sensitivity to global DSBs induced by zeocin (Figure 2, Table 2). As such, we characterize the proteins encoded by these genes as being novel DNA damage response proteins. The candidate proteins that were enriched at the DSBs, but whose mutation did not render sensitivity to DNA damage (Figure 2), presumably perform non-essential and / or redundant functions during DSB repair, or may play roles in the fidelity of repair.

Some of the novel DNA damage response proteins are specific to DSB repair, while others are required for general stress responses

To provide further mechanistic insight into the function of the novel DNA damage response proteins, we asked whether their role was specific to DSBs or general for multiple forms of stress. The other stresses tested include the ribonucleotide reductase inhibitor hydroxyurea (HU) that results in reduced DNA replication due to depleted nucleotide pools, the DNA alkylating agent methyl methane sulfonate (MMS), heat which activates the integrated stress response, the oxidative stress inducer hydrogen peroxide (H₂O₂), and the UV damage mimetic agent 4-nitroquinoline 1-oxide (4-NQO). We found that the candidate mutants exhibit distinct stress sensitivity profiles (Figure 3, Table 2). For example, *def1Δ* is sensitive to all the stresses, whereas other mutants like *ACS2* DAmP, are sensitive to only the radiomimetic zeocin. These results indicate that while some of these novel

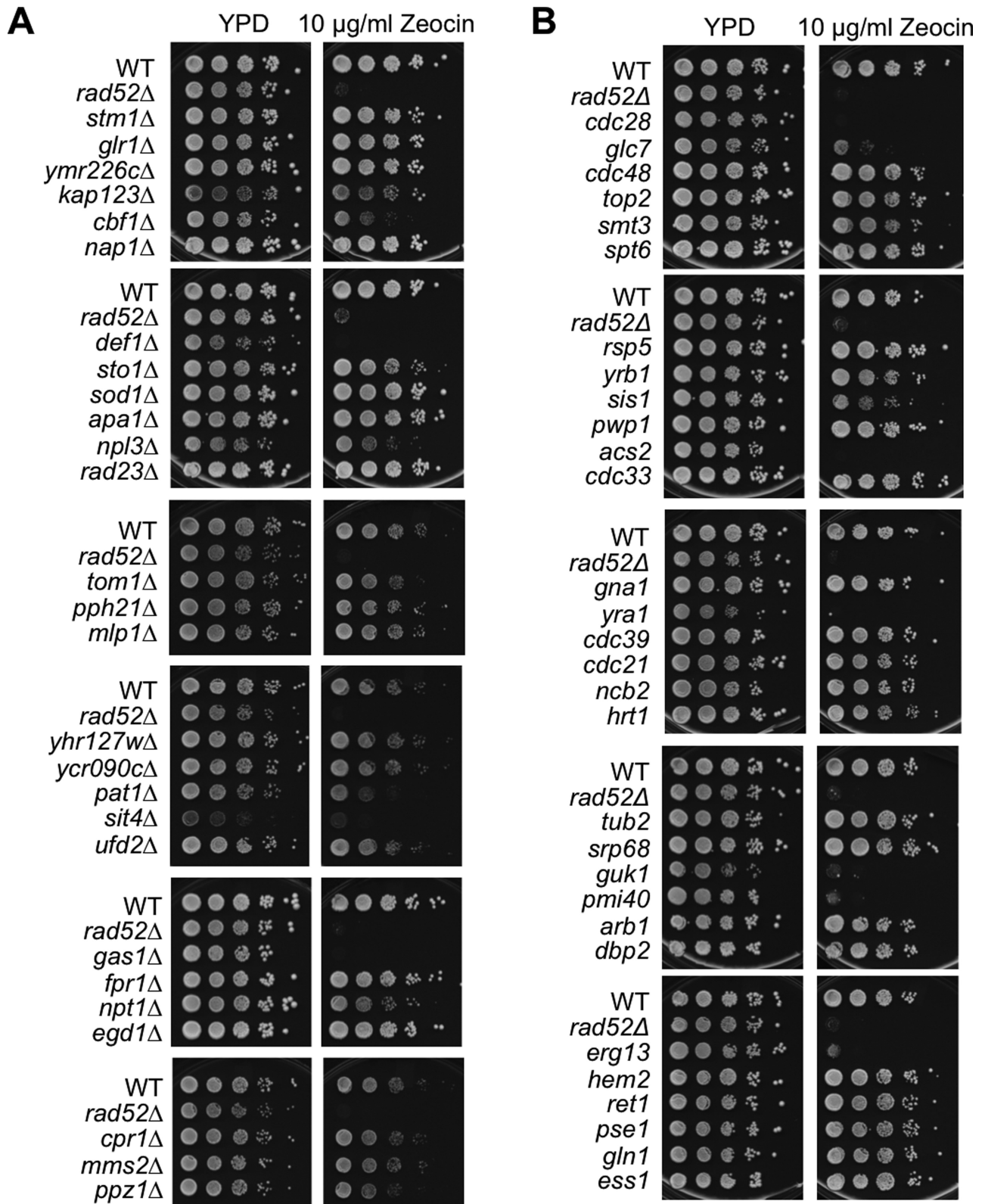


Figure 2. Mutants of multiple candidate genes whose protein products were enriched at the DSB show sensitivity to the radiomimetic zeocin. (A) Deletion mutants of non-essential candidate genes including *CBF1*, *DEF1*, *NPL3*, *TOM1*, *PAT1*, *SIT4*, *GAS1*, *NPT1* and *PPZ1* show sensitivity to zeocin. 10-fold serial dilutions on YPD or plates supplemented with zeocin. The *rad52*Δ mutant served as a positive control for DSB sensitivity. (B) DAMP mutants of essential candidate genes including *SIS1*, *ACS2*, *YRA1*, *GUK1*, *PMI40* and *ERG13* show sensitivity to zeocin. *CDC28* and *GLC7* DAMP mutant are positive controls for essential proteins identified adjacent to the HO lesion with known roles in the DNA damage response.

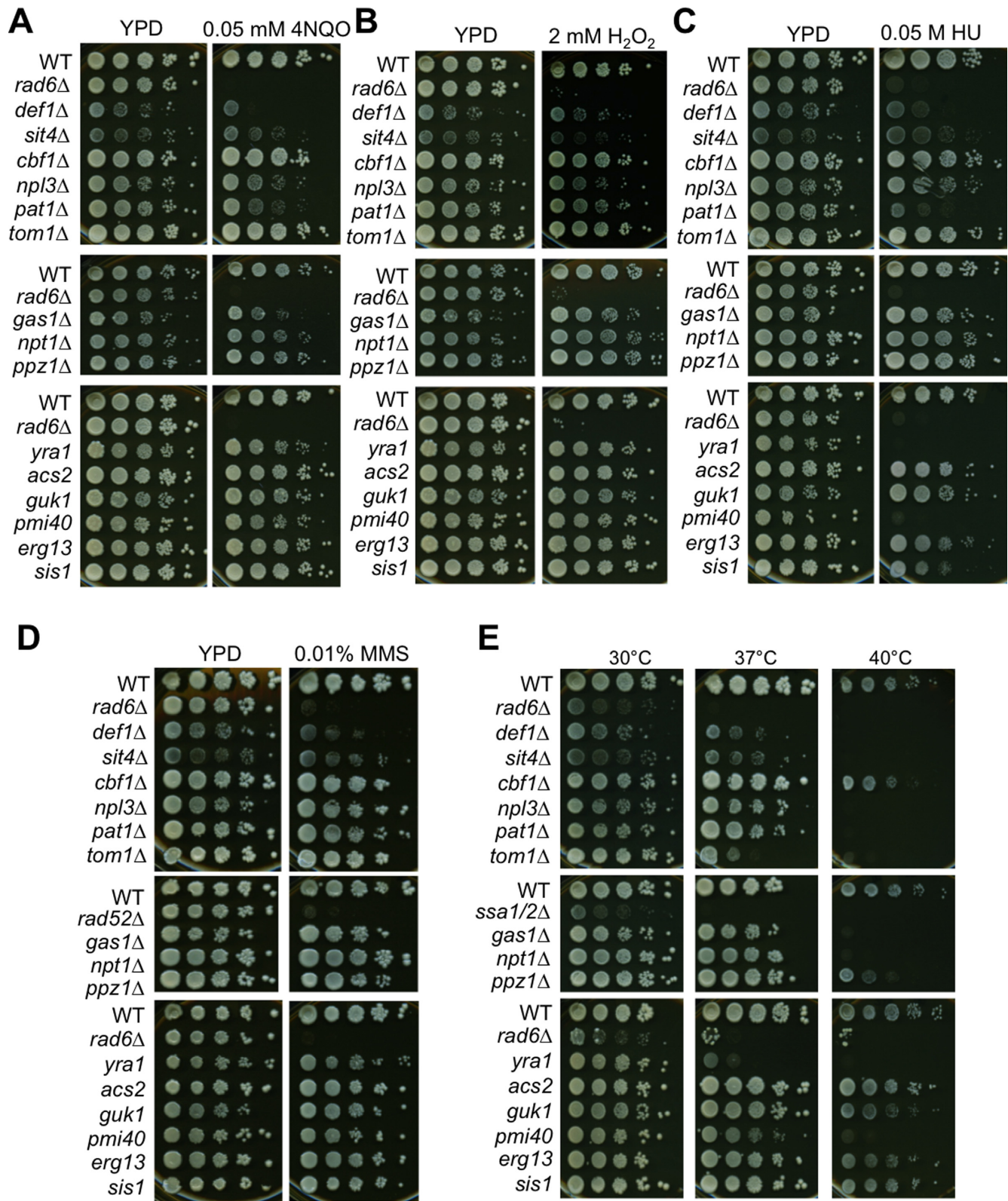


Figure 3. Profiling of the zeocin-sensitive candidate mutants' sensitivity to other types of stress. (A) Serial dilution analyses of the indicated strains, as in Figure 2. The *rad6Δ* mutant is a positive control for 4-NQO sensitivity. (B) *yap1Δ* mutant is a positive control for H₂O₂ sensitivity. *rad52Δ* is a positive control for (C) HU and (D) MMS sensitivity. (E) *ssa1/2Δ* is a positive control for heat sensitivity.

Table 2. Summary of stress sensitivity of candidate yeast mutants

Yeast Strain	Zeocin	4NQO	H2O2	HU	MMS	Heat	HO
<i>def1</i> Δ	++++	+++	+	++	++	++++	–
<i>sit4</i> Δ	+++	+	+++	–	–	++++	+
<i>cbf1</i> Δ	++	–	–	–	–	+	–
<i>npl3</i> Δ	++	+	+	–	–	++++	N.D.
<i>pat1</i> Δ	++	+	–	++	–	++++	–
<i>tom1</i> Δ	+	–	–	–	–	++++	+
<i>gas1</i> Δ	++++	++	–	–	–	++++	–
<i>npl1</i> Δ	+	–	–	–	–	++++	–
<i>ppz1</i> Δ	+	–	–	–	–	++	–
<i>YRA1 DAmP</i>	++++	–	–	++++	–	++++	N.D
<i>ACS2 DAmP</i>	++++	–	–	–	–	–	N.D
<i>GUK1 DAmP</i>	+++	–	–	–	–	–	N.D
<i>PMI40 DAmP</i>	+++	–	–	++++	–	+++	N.D
<i>ERG13 DAmP</i>	+++	–	–	–	–	–	N.D
<i>SIS1 DAmP</i>	+	–	–	+	–	–	N.D
Wild type	–	–	–	–	–	–	–

Sensitivity degree: +++++ > ++++ > +++ > ++ > +

No sensitivity: –

N.D: not determined

DNA damage response proteins are involved specifically in the response to DSBs, others are part of a general DNA damage response, while others are more broadly involved in cellular stress responses.

Elevated temperature leads to an HR defect, while the heat shock proteins Ssa1/2 promote the DNA damage response at normal temperatures

We were surprised to find that so many of our mutants were sensitive to both zeocin and heat (Table 2). In mammals, hyperthermia causes defects in HR (28–30), but the molecular details are not clear and this has not been examined in yeast. We asked whether heat itself may render yeast sensitive to DSB-inducing damaging agents. As a control to establish that we had achieved heat shock conditions, we included a double deletion mutant of the heat shock proteins Ssa1 and Ssa2 because growth at elevated temperatures requires Ssa1/2, as seen in Figure 4A. Indeed, we found that the resistance of wild type yeast to zeocin is greatly reduced at elevated temperatures, suggesting that heat causes a defect in DSB repair (Figure 4A). In addition to zeocin sensitivity, we found that heat reduced viability of wild type yeast 100-fold upon induction of the HO endonuclease that generates a single DSB that is repaired by homologous recombination (Figure 4B and C). This suggests that heat causes a defect in homologous recombination. Furthermore, in the single strand annealing strains, heat elevated the sensitivity to induction of an HO lesion that is repaired by single strand annealing (Figure 4C). These results indicate that heat compromises an early stage in homologous recombination, which would explain the heightened heat sensitivity of the many deletion mutants that are also sensitive to zeocin (Table 2).

Although we originally included the *ssa1*Δ/*ssa2*Δ double mutant as a control for heat shock because Ssa1/Ssa2 are essential at elevated temperature, we unexpectedly found that deletion of *SSA1/2* greatly reduced yeast survival after exposure to radiomimetics at the normal growth temperature of 30°C (Figure 4A). This result indicates that Ssa1/2 are

required for survival after exposure to DSBs at normal temperatures. In agreement, their mammalian homolog HSP70 proteins protect the genome against genomic instability after irradiation (31), yet their molecular role in DSB repair is unclear. Deletion of *SSA1/2* also led to sensitivity to the HO lesion that is repaired by single strand annealing (Figure 4C). These results indicate that Ssa1/2 plays a role in either an early stage of homologous recombination or survival after DSB repair.

To determine whether the novel DNA damage response proteins were sensitive to a single DSB in addition to global DNA damage, we induced a single DSB at the *MAT* locus. A *rad52*Δ mutant was included as a positive control for DNA damage sensitivity. Out of all the non-essential novel DNA damage response proteins, only Sit4 and Tom1 were required for resistance to the galactose-inducible HO endonuclease that cuts at the *MAT* locus (Table 2, Figure 5A). We were unable to measure the role of the essential novel DNA damage response proteins to repair of the HO lesion, since the available DAmP mutants are all derived from a *MATa* background that has a ‘*MAT-stuck*’ mutation (32) preventing the HO endonuclease from cleaving the *MAT* locus.

The DNA damage sensitivity of *tom1* does not reflect a role in either DSB repair or checkpoint recovery

Given that we had found that Tom1 localizes to DSBs and that *tom1*Δ mutants are sensitive to both zeocin (Figure 2A) and induction of the HO lesion at *MAT* (Figure 5A), we focused on its mechanistic role in the DSB response. *TOM1* encodes a HECT E3 ligase that is involved in transcriptional regulation through histone acetylation (33) and degradation of excess histone proteins (34). However, Tom1 has not been directly implicated in the DNA damage response previously. Failure to grow following exposure to DNA damage can be for many reasons including failure to repair the DNA break or failure to inactivate the DNA damage checkpoint after DNA repair, via a process called checkpoint recovery (35). We asked whether *tom1*Δ mutants could repair the HO

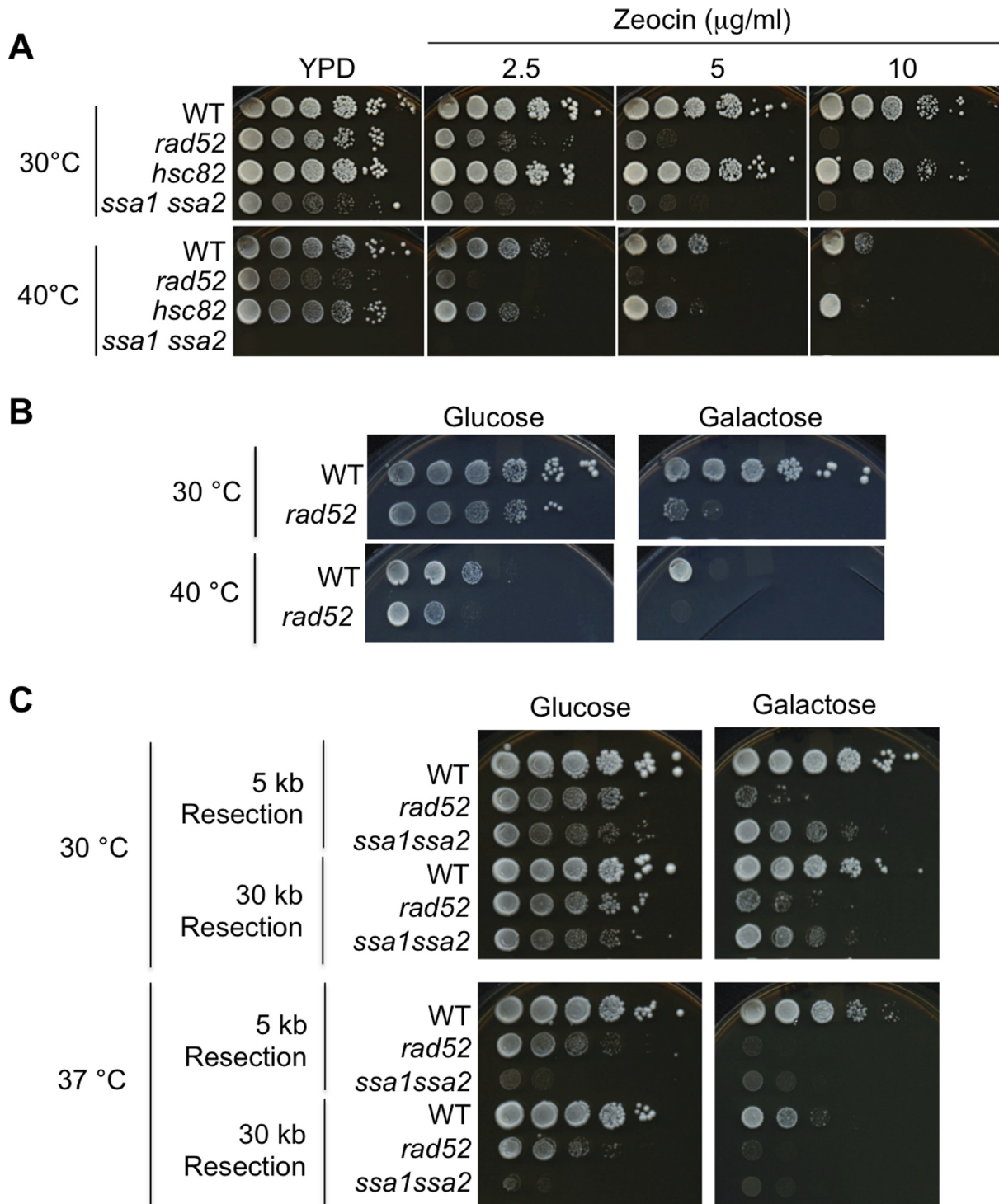


Figure 4. Hyperthermia or deletion of the yeast HSP70 encoding genes (*SSA1/2*) leads to a defect in homologous recombination. (A) Yeast strains (BY4741 derivatives) with the indicated gene deletions were 10 fold serially diluted and equal amounts plated onto control media (YPD) or media with the indicated amounts of the radiomimetic zeocin. *HSC82* encodes the yeast Hsp90 protein, and appears to play little role in DSB repair. (B) Equal amounts of the wild type (BY4742) or isogenic *RAD52* deleted yeast strains carrying the pGAL1-HO gene, were 10-fold serially diluted onto media containing glucose or galactose at the indicated temperatures. (C) The 10-fold increased sensitivity of the 30kb *ssa1 ssa2* strain (PWY061) versus the 5 kb resection strain (PWY062) to galactose indicates a defect in either resection or the DNA damage response. The 30 kb WT strain, 30 kb *rad52*Δ strain, 5 kb WT strain, and 5kb *rad52*Δ strain are YMV2, YMV37, YMV45 and YMV46, respectively. Similarly, there is a 100-fold increased sensitivity of the 30 kb versus 5 kb strain to hyperthermia on galactose plates.

lesion at *MAT* using the same PCR assay used in Figure 1C. The cutting and repair in the *tom1* Δ mutant was identical to the WT strain (Figure 5B) indicating that Tom1 is not required for repair of the HO lesion at *MAT*.

To investigate whether Tom1 was involved in checkpoint recovery after DSB repair, we used another inducible HO system where the DSB is repaired by single-strand annealing (SSA). In the SSA system (36), the HO lesion is induced between two repeated sequences spaced 30 kb apart on the same chromosome, in the YMV2 strain. Repair of this HO lesion occurs following 30kb of resection and this temporal delay necessitates activation of the DNA damage checkpoint. As such, sensitivity to induction of the HO lesion that is repaired by SSA, in a strain that is otherwise proficient for DSB repair, is indicative of delayed DNA damage checkpoint recovery. We found that the *tom1* Δ mutant was not significantly more sensitive than the WT cells to induction of the HO lesion that is repaired by SSA (Figure 5C), suggesting that Tom1 does not play a role in checkpoint recovery. In addition, the dephosphorylation kinetics of the effector checkpoint kinase Rad53 (37), indicative of inactivation of the DNA damage checkpoint, was identical in the *tom1* Δ mutant and WT strain following transient treatment with zeocin (Figure 5D). Taken together, these data indicate that the sensitivity of *tom1* mutants to global DSBs and a DSB at the *MAT* locus does not reflect a role for Tom1 in either repair of DSBs or DNA damage checkpoint recovery.

Sit4 is required for recovery from the DNA damage checkpoint after DSB repair

SIT4 encodes a protein phosphatase with similarity to human PP6 (38), and has not been directly implicated in the DNA damage response previously. To determine whether the sensitivity of the *sit4* Δ mutant to HO endonuclease (Figure 2A) was due to a defect in DNA repair, we examined repair of the HO lesion at *MAT* directly. While the *sit4* Δ mutant showed a delay in the appearance of DNA repair products, this was due to the delayed and reduced HO cutting observed in the *sit4* Δ mutant (Figure 5B). Given that Sit4 was not required for DNA repair *per se*, we wanted to test if it played a role in checkpoint recovery. Unfortunately, we were unable to delete *SIT4* in the SSA strain background. This is probably because of the synthetic lethal interaction with *SSD1* (Suppressor of *SIT4* deletion) (39), given that *SSD1* is mutant in the strain background used to create the SSA strain (36).

However, when we tested the kinetics of dephosphorylation of Rad53 following a transient zeocin treatment, it was apparent that dephosphorylation in the *sit4* Δ strain was approximately 4 hours slower than the WT strain (Figure 5D). Importantly, the *sit4* mutant did not have a detectable defect in DSB repair following induction of global DNA damage with zeocin, as reflected in the smearing of the chromosomal bands resolved by PFGE and their subsequent restoration after washing out zeocin (Figure 5E). Taken together, these data suggest that localization of Sit4 to DSBs reflects its role in checkpoint recovery after DSB repair.

Def1 promotes repair of global DSBs, independent of any putative role in degrading RNA polymerase II

DEF1 promotes transcription-coupled repair (TCR) via its role in degradation of RNA polymerase II (RNA pol II) at genes with single-strand DNA lesions (40). We found Def1 localizing to DSBs and a *def1* Δ mutant had sensitivity to zeocin (Figure 2A). However, the *def1* Δ mutant was not particularly sensitive to induction of the HO lesion at *MAT* (Figure 6A) beyond having slow growth, which was also seen on glucose plates. In agreement, there was no kinetic difference in the repair of the HO lesion at *MAT*, even though less DSBs were induced in the *def1* Δ mutant (Figure 6B; Supplementary Figure S3). Given that Def1 promoted TCR via its role in degrading RNA pol II (40) and given that it has been reported that RNA pol II is degraded after DSB damage (41) we asked whether Def1 specifically promotes DSB repair within highly-transcribed genes. To do this, we generated a strain where the HO site was inserted into the *ADH1* gene and the HO site at *MAT* was deleted. We found that the *def1* Δ mutant was not sensitive to induction of an HO lesion within the *ADH1* gene (Figure 6C). Furthermore, in our hands, deletion of *DEF1* had no effect on RNA pol II levels following treatment with global DNA damaging agents (Supplementary Figure S3). As such, Def1 is not required for the repair of a unique HO lesion by HR, yet promotes resistance to global DSB induction.

Given that we did not detect a role for Def1 in either repair or survival after induction of a single DSB made by the HO endonuclease, we focused on its role in resistance to global DSBs (Figures 6A and 6C). We examined the ability of the *def1* Δ mutant yeast to repair global DNA damage by PFGE analysis of yeast chromosomes. While the chromosomes became intact in WT cells by ~5–6 h after recovering from zeocin treatment, the restoration of the intact chromosomal profiles was delayed in *def1* Δ mutant cells (Figure 6D). In agreement with the delayed repair of zeocin-induced DSBs in the *def1* Δ mutant cells, dephosphorylation of Rad53 was delayed several hours after removal of zeocin in the *def1* Δ mutant cells compared to wild type cells (Figure 6E, Supplementary Figure S3C). Taken together, these data indicate that Def1 plays a role in global DSB repair.

Yra1 plays a major role in DSB repair

YRA1 encodes an essential protein involved in mRNA export (42). We found Yra1 localizing to DSBs and a DAMP hypomorph of Yra1 was highly sensitive to zeocin (Figure 2B). As mentioned earlier, we were unable to generate an HO endonuclease-induced DSB at the *MAT* locus in the DAMP (*MATa*) mutants, due to the presence of a mutation at the *MAT* HO site that is uncuttable by the HO endonuclease in the DAMP mutant collection. Therefore, in order to determine whether Yra1 contributed to repair of the HO-induced DSB at the *MAT* locus, we used an *YRA1* anchor-away (AA) mutant (43). An AA mutant allows nuclear depletion of the protein of interest upon rapamycin addition. There are two major components in the *YRA1* AA mutant (YCL003) that we used in our study: one is the cytoplasmic anchor protein fused to FKBP12, and the other is the target protein fused to FRB. Since the presence of rapamycin leads to the formation of a ternary complex con-

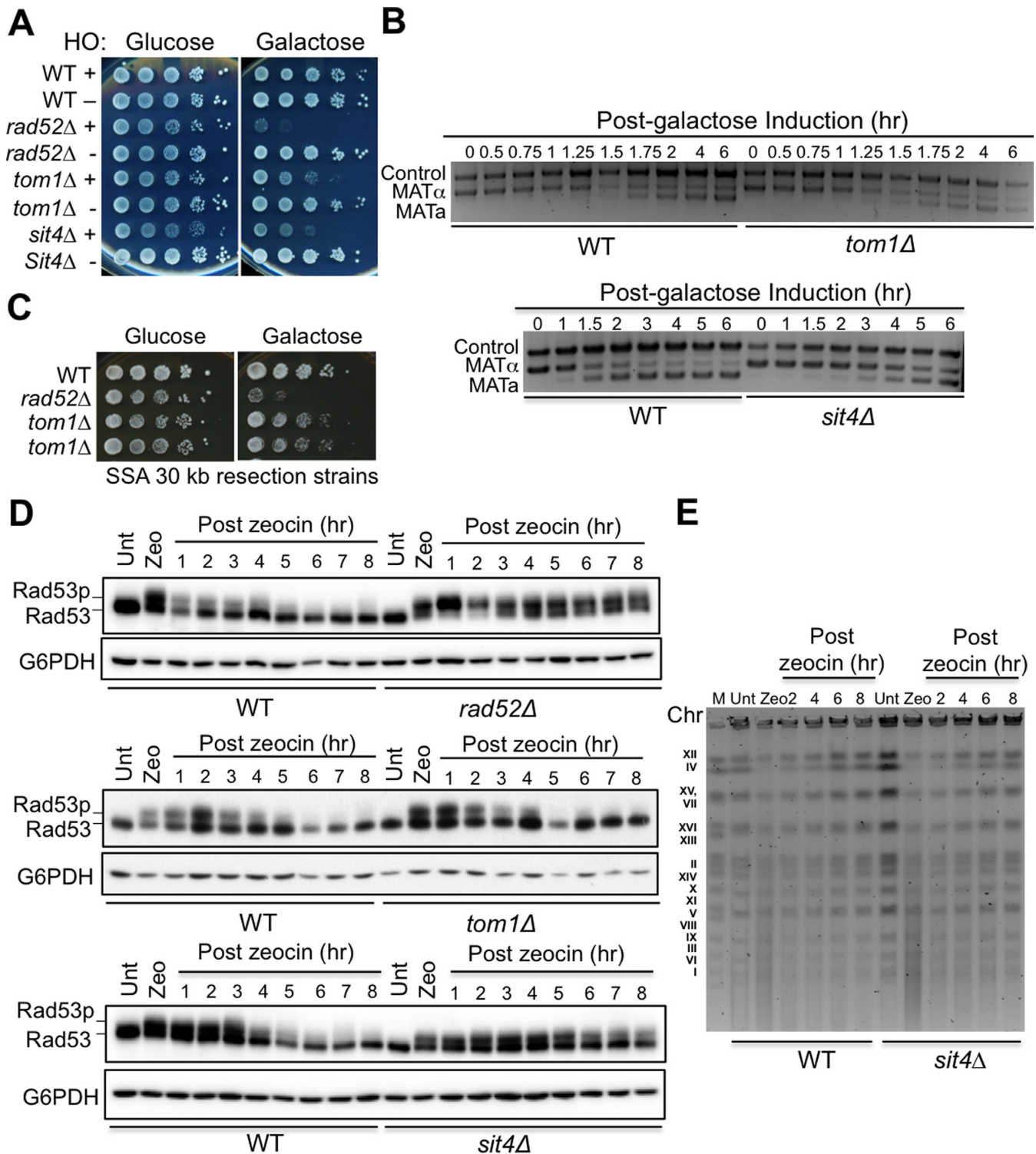


Figure 5. *Sit4* promotes checkpoint recovery. (A) *SIT4* and *TOM1* deletion mutants show sensitivity to constant induction of an HO-induced DSB at the *MAT* locus. Ten fold dilution analysis of the indicated strains (BY4742 wild type or mutants from the isogenic deletion library) containing either *pRS316* '- HO' or *pGAL-HO* '+ HO' on SC-uracil media containing either glucose or galactose. (B) Neither *SIT4* nor *TOM1* are required for repairing an HO-induced DSB at the *MAT* locus. Cutting and repair assay as described in Figure 1C, using WT or the indicated mutant strains bearing *pGAL-HO* that have been used in A. (C) *TOM1* deletion mutant (PWY069) does not show sensitivity to the induction of a single DSB that is repaired by SSA. The WT and *rad52Δ* strains are YMV2 and YMV37, respectively. (D) Deletion of *SIT4* but not *TOM1* delays dephosphorylation of Rad53 after removal of zeocin ('Zeo'). *rad52Δ* served as a positive control for persistent Rad53 phosphorylation after release from a transient DSB-inducing treatment. The WT strain was BY4741, and the indicated mutant strains were all from the BY4741 derived deletion library. 'Unt' indicates untreated. G6PDH serves as a loading control. (E) A *sit4Δ* mutant is proficient for repairing chromosomal damage induced by zeocin treatment. The WT strain was BY4741, and the *sit4Δ* strain was from the BY4741 derived deletion library. Chromosomal DNA was subjected to pulsed field gel electrophoresis (PFGE), from the indicated time points after removal of zeocin. 'Unt' indicates untreated, 'Zeo' indicates a sample before washing out zeocin, and 'M' indicates yeast chromosomal DNA marker.

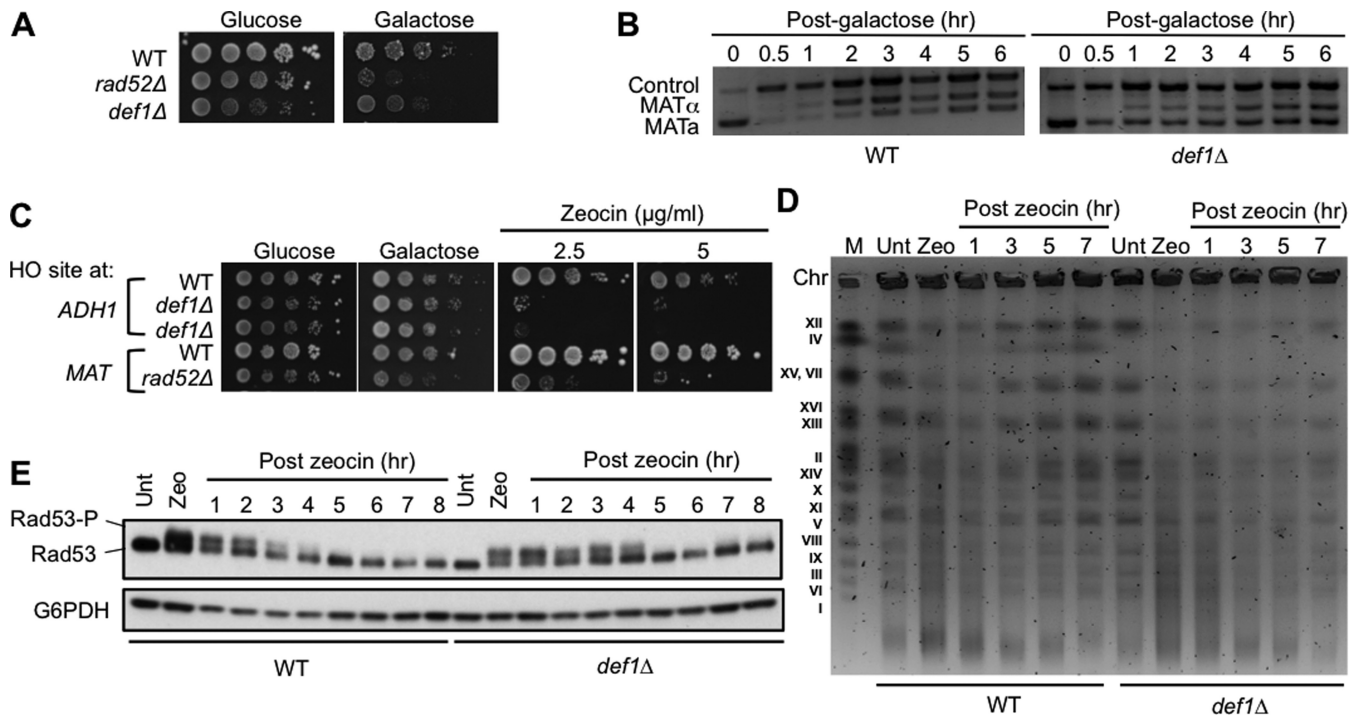


Figure 6. *Def1* promotes DSB repair following radiomimetic treatment. (A) Deletion of *DEF1* confers little (if any) sensitivity to HO-induced DSBs at the *MAT* locus, measured using strain BAT009 (WT), BKD0665 (*rad52Δ*) and PWY033 (*def1Δ*). (B) *DEF1* null mutant does not have a DSB repair defect at the *MAT* locus, using the assay shown in Figure 1C and strains BAT009 (WT) and PWY033 (*def1Δ*). (C) Deletion of *DEF1* does not confer sensitivity to an HO lesion within the *ADH1* gene. Serial dilution analysis of strains PWY081 (*ADH1*-HO site, WT), PWY099 (*ADH1*-HO site, *def1Δ*), BAT009 (*MAT* locus, WT) and BKD0665 (*MAT* locus, *rad52Δ*) onto plates containing the indicated supplements. (D) A *def1* null mutant shows a defect in chromosomal repair after release from transient zeocin treatment. The PFGE procedures were the same as described in Figure 5E, using strains W303-1A (WT) and JSY568 (*def1Δ*). (E) A *def1* null mutant has a delay in dephosphorylating Rad53 after release from zeocin, performed as in Figure 5D using strains W303-1A (WT) and JSY568 (*def1Δ*).

taining FRB, FKBP12 and rapamycin, the target (Yra1-FRB) and anchor proteins (Rpl13A-FKBP12) are retained in the cytoplasm upon rapamycin addition. In addition, the shuttling of the ribosomal protein Rpl13A from the nucleus to cytoplasm during ribosomal maturation enables the anchor protein to capture the target protein. *TOR1* is deleted from the AA strains so that the altered growth is not due to sensitivity to rapamycin *per se*. In order to study the essential Yra1 protein in a growth assay, it was only transiently depleted from the nucleus by adding rapamycin to the liquid cultures for 1 hour, followed by plating onto media lacking rapamycin. We confirmed that rapamycin-mediated Yra1 depletion from the nucleus confers the *YRA1* AA strain, but not the wild type AA strain, sensitive to zeocin (Figure 7A, Supplementary Figure S4A). Zeocin sensitivity upon Yra1 depletion was apparent in asynchronous cultures, and was more apparent in cells synchronized in G₁ phase with alpha factor or in G₂/M phase with nocodazole. When we examined the kinetics of the repair of the HO lesion at the *MAT* locus, we found no difference for the rapamycin-treated *YRA1* AA cells (Figure 7B). Confirming efficient depletion of Yra1 from the nucleus, we observed Yra1 was cytoplasmic after rapamycin treatment (Supplementary Figure S4B). Given that there was no apparent role for Yra1 in repair of the HO lesion, yet the Yra1 DAMP hypomorph had striking sensitivity to zeocin, we examined global DSB repair more closely. When examining the repair of global

DSBs by PFGE analysis, we observed a striking defect in DSB repair in the Yra1 hypomorph (Figure 7C), where the *YRA1* DAMP allele leads to an 8 fold reduction in mRNA levels (Supplementary Figure S5). Consistent with a central role of Yra1 in DSB repair, the DNA damage checkpoint was persistently maintained in an active state following washing out the zeocin (Figure 7D). These data uncover a profound role for Yra1 in global DSB repair.

DISCUSSION

Although the DSB repair pathways have been intensively studied, we still don't totally understand their interplay with transcription, the DNA damage checkpoint and their function in the chromatin context within the cell. Because the DSB response pathways are highly conserved from yeast to larger eukaryotes, dissecting the molecular mechanisms underlying the cellular response to DSBs in yeast facilitates our understanding of the complex regulatory events that occur in mammals. Using an unbiased proteomics approach, we have discovered numerous novel histone PTMs occurring at the site of DSB repair and novel proteins that are required for different aspects of the DNA damage response.

We identified numerous histone PTMs enriched around a yeast DSB that we are not aware of being previously implicated in DSB repair. These include H2A K4ac K7ac, H2B K6ac K11ac, H2B K16ac, K17ac and H3 K122ac K125me. Further validation of the roles of these histone

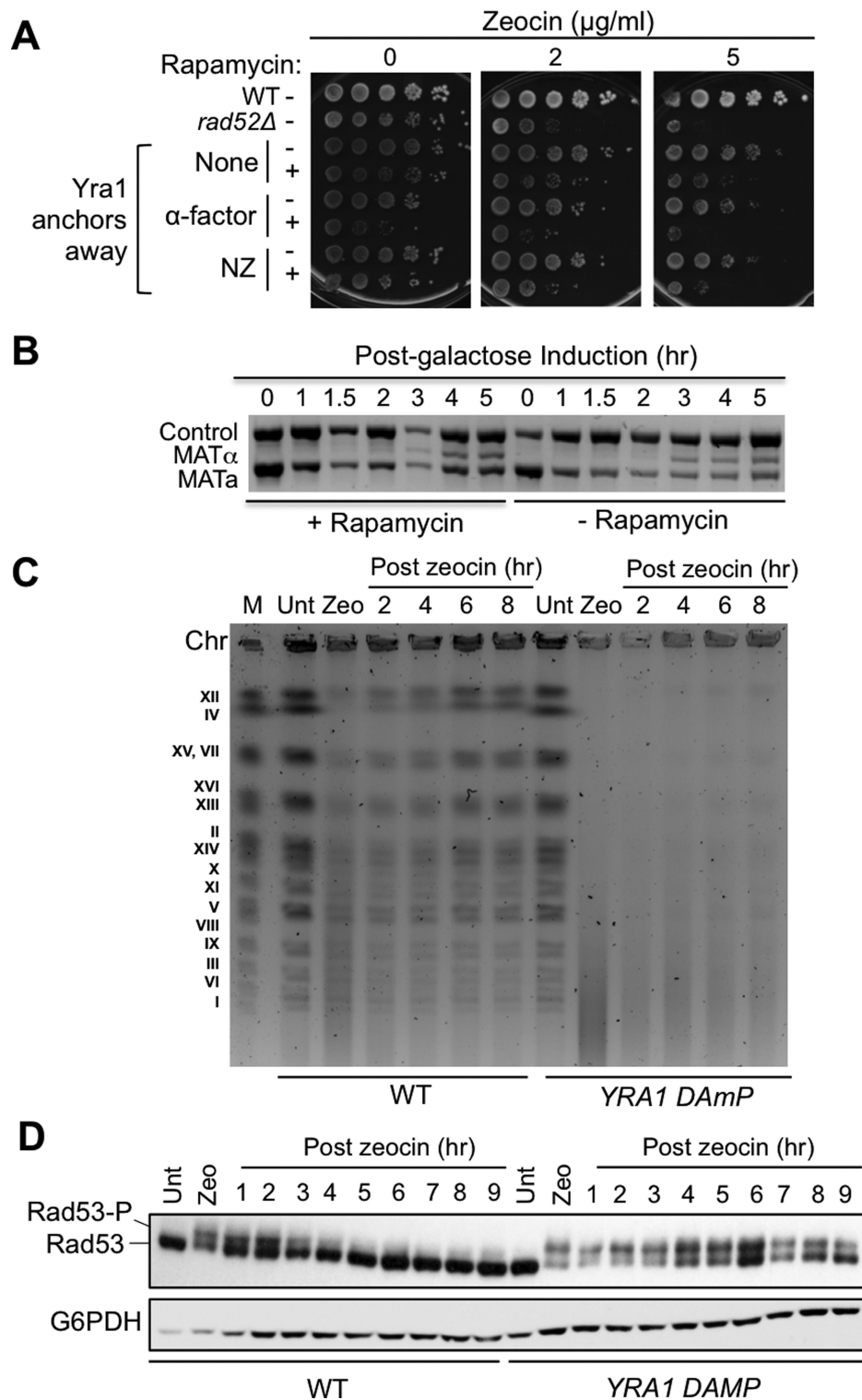


Figure 7. Yra1 is required for DSB repair. (A) The yeast Yra1 anchors-away strain YCL003 is sensitive to zeocin after rapamycin induction. '-' and '+' indicate whether 1 h of rapamycin (1 μg/ml) was added to the cell culture before the serial dilution assay. Cells with or without rapamycin treatment were washed in YPD twice before being serially diluted. The YPD agar plates were rapamycin free and contained the indicated amount of zeocin. The strains BAT009 (WT) and BKD665 (*rad52Δ*) served as negative and positive controls, respectively, for zeocin sensitivity. (B) Depletion of Yra1 from the nucleus did not result in a defect in repairing the HO-induced DSB at the *MAT* locus measured as in Figure 1C, using strain YCL003 bearing the plasmid *pGAL-HO*. Two groups of cells were used in this experiment: one where rapamycin and galactose were both added at time 0 (T0), the other where only galactose was added at T0. For both groups of cells, glucose was added at T2 to allow repair. (C) *YRA1* DAMP mutant (from the *MAT* aDAMP library) is defective in restoration of intact chromosomes after a transient zeocin treatment. The WT strain was BY4741, from which the *MAT* aDAMP library was generated. The PFGE analysis was as described in Figure 5E. (D) *YRA1* DAMP mutant is defective in dephosphorylating Rad53 after release from a transient zeocin treatment. Strains used were the same as in 7C.

PTMs during the DNA damage response awaits the development of specific antibodies. We also identified numerous histone PTMs enriched around DSBs, that were previously known to impact the DSB repair process. This validates our approach and indicates that these histone PTMs most likely function in a local manner to influence the DSB response. Interestingly, we did not identify H2A phosphorylation on serine 129 (γ H2A), a well-known DNA damage response histone PTM, as either depleted, enriched or unchanged at a DSB site. i.e. it was not detectable. This is consistent with the reported very low levels of γ H2A immediately 1–2 kb around a DSB (44). Noteworthy, and consistent with the temporal coupling of histone removal with DNA resection, and DNA repair with histone replacement (23), we did not observe core histone depletion from the dsDNA around a DSB by the ChAPs method. We also identified a histone PTM that had not been reported before, to our knowledge. This was H3 K125me. Given that ubiquitination of H3 K125 promotes chromatin assembly (45), H3 K125me around a DSB would presumably block K125 ubiquitination, which would be desirable to promote chromatin disassembly during HR repair (23). It will be interesting to determine the function of this new histone PTM in general, and during DSB repair specifically, in the future.

While classical forward genetic screens in yeast have been instrumental in identifying the most critical components of the DNA damage response, it is unlikely that saturation across the genome has been achieved. Accordingly, systematic analyses of the yeast deletion collections for sensitivity to a variety of DNA damaging agents identified many new genes involved in the DNA damage response (46). However, we considered that a proteomic approach based on protein localization to a single DSB would yield new players in the DNA damage response for the following reasons: (i) Essential genes were not studied in the systematic analyses, (ii) some non-essential genes are missing from the deletion collections while other genes have not been deleted but the deletion marker inappropriately inserted elsewhere in the genome, (iii) 7–15% of phenotypes observed in the deletion collection are due to disrupting the neighboring gene, via neighboring gene effects (47) while secondary mutations have been found to often cause the phenotype in deletion collection strains, rather than the knockout allele (estimated to be 6.5% for growth) (48), (iv) cross contamination and aneuploidy accumulate in deletion collection libraries due to manipulation and selective pressure (49), (v) the systematic analyses were often performed in diploid not haploid yeast, (vi) the systematic analyses were based on growth, requiring generations of cell cycles, while we were specifically looking during the DNA repair process *per se*, and finally (vii) to our knowledge, none of the systematic analyses were performed in response to induction of an HO lesion, as was the case in our study.

Using our unbiased proteomics approach, we identified 108 proteins enriched around a DSB undergoing homologous recombination that have not been previously implicated in DSB repair. Among the genes we tested, the non-essential *CBFI*, *DEF1*, *NPL3*, *TOM1*, *PAT1*, *SIT4*, *GAS1*, *NPT1* and *PPZ1* genes and the essential *SIS1*, *ACS2*, *YRA1*, *GUK1*, *PMI40* and *ERG13* genes promoted yeast resistance to zeocin (Figure 2, Table 2). Some of these genes

were additionally required for resistance to other forms of stress (Figure 3) indicating that they play general roles in the stress response.

Hyperthermia, the most efficient chemo- and radio-sensitizer known, is being used in clinical settings for inhibiting tumor growth (50,51). Several laboratories have reported that hyperthermia inhibits DNA damage repair by HR in mammals (28–30). Driven by the finding that many of our novel DNA damage response proteins were sensitive specifically to zeocin and heat, but not other damaging agents (Table 2), we investigated whether elevated temperature leads to defects in DSB repair, which would explain why our yeast mutants were hypersensitive to heat. Our data suggested this is also the case in yeast, since cells grown at elevated temperature are sensitive to zeocin and to induction of the HO lesion that is repaired by homologous recombination or single strand annealing (Figure 4). Furthermore, cells lacking the yeast equivalents of human HSP70 proteins, *Ssa1* and *Ssa2*, were hypersensitive to the radiomimetic zeocin and induction of the HO lesion that is repaired by homologous recombination or single strand annealing.

We chose to further investigate the function of four of the novel DNA damage response proteins that we found in the ChAP-MS: *Sit4*, *Tom1*, *Def1* and *Yra1*. We found that *Sit4* is not required for DSB repair, but is required for checkpoint recovery (Figure 5). Yeast *Sit4* is similar to the human phosphatase PP6 (52). In agreement with our proposed role for yeast *Sit4* in checkpoint recovery, depletion of PP6 in human cells increases sensitivity to ionizing radiation (IR), due to a delay in release from the DSB-induced checkpoint, and caused a defect in dephosphorylation of γ H2AX after IR (53). Also, there is no apparent DSB repair defect in PP6-depleted cells, consistent with the lack of a DSB repair defect in yeast *sit4* mutants (Figure 5). PP6 interacts with the NHEJ protein DNA-PK leading to a model in which DNA-PK helps to recruit PP6 to DSBs to facilitate the dephosphorylation of γ H2AX and checkpoint recovery (53). Our findings on *Sit4* suggest that the role of this family of phosphatases during checkpoint recovery is conserved from yeast to human.

Mechanistically, how are *Sit4* and PP6 promoting checkpoint recovery? It is unlikely that *Sit4* dephosphorylates γ H2A directly given that *Pph3* is already known to be the γ H2A phosphatase (17). Moreover, the persistent Rad53 phosphorylation in the *sit4* mutant suggests that Rad53 dephosphorylation is also influenced by *Sit4*. Noteworthy, *Mec1*, the yeast counterpart of human ATR, is responsible for phosphorylating both H2A and Rad53 during the DNA damage response, making inactivation of *Mec1* a likely indirect target of *Sit4*, in order to enable dephosphorylation of Rad53 and γ H2A. A role for *Sit4* in down-regulating *Mec1* activity after DSB repair to promote checkpoint recovery could potentially occur through *Pkc1*. The rationale for this suggestion is because *Pkc1* is required for *Mec1* and *Tel1* (the yeast equivalent of human ATM) activity in response to DSBs (54). Likewise, the human counterpart of *Pkc1*, *PKC δ* , is also required for activation of the DNA integrity checkpoint (54). Meanwhile, *Sit4* is required for down-regulating *Pkc1* activity, seeing as *Pkc1* is overactive in the absence of *Sit4* (55). As such, *Sit4* could potentially dephosphorylate

Pkc1, which is known to be phosphorylated by the central checkpoint kinases potentially in a feedback loop (54), in order to inactivate Mec1 to allow checkpoint recovery.

We found that although the Tom1 HECT3 E3 ligase protein localizes to DSBs, it is not required for checkpoint recovery or DSB repair. As such, it seems likely that the excess histones that are present in the *tom1* mutant (34) themselves are toxic to the cells following DNA damage, leading to the growth defect observed with zeocin and upon induction of a single HO lesion at *MAT*. Intriguingly, we did not observe sensitivity to the HO lesion induced in the SSA assay system in the *tom1* mutant. However, one key difference between the HO at *MAT* and the HO induced in the SSA system is that the HO at *MAT* is continuously cleaved and repaired over the three days of growth, while the HO in the SSA system is cut and repaired only once, because the repair uses an HO sequence containing a mutation that prevents recutting. The fact that Tom1 was recruited to DSB breaks suggests that the role of Tom1 in ubiquitinating the histones likely occurs at the site of repair (34), perhaps promoting degradation of the histones as they are removed from around the DSB lesion. Indeed, we observed a drastic loss of histones from chromatin following the induction of global DSBs in a dose responsive manner (Supplementary Figure S6), as has been observed very recently by others (56).

We found Def1 to be recruited to DSBs and to promote repair of global DSB damage. *DEF1* was shown to be required for the degradation of the largest subunit of RNA pol II in response to UV damage (40). In this way, RNA pol II is removed from genes with UV-induced DNA lesions to enable their transcription-coupled repair. Another known degradation target of *DEF1* is Pol3, which is the catalytic subunit of DNA polymerase δ (57). This Def1-mediated Pol3 degradation after UV irradiation was suggested to allow the translesion synthesis polymerase to take the place of Pol3 and mediate error-prone DNA synthesis (57). However, we do not consider that Def1 is promoting DSB repair via a role in degradation of RNA pol II after DSB damage, because we did not observe any role for Def1 in repair of a DSB within a highly transcribed gene (Figure 6C). Furthermore, we observed no effect of *DEF1* deletion on RNA pol II levels after inducing DSB damage (Supplementary Figure S3). Perhaps the role of Def1 in repair of global DSBs is related to the function of *DEF1* in telomere maintenance (58), which depends on the NHEJ machinery. As such, a role for Def1 related to NHEJ could explain the lack of any HR defects during HO repair in the *def1* mutant, while there was reduced global DSB repair (Figure 6). Def1 has also been implicated in meiotic DNA processing (59) which could be related to the role we found for Def1 during DSB repair. We propose that Def1 coordinates the degradation of specific protein(s) (yet to be determined) at the site of DSB repair that promotes efficient DSB repair.

YRA1 mutants were as sensitive to DSBs as yeast lacking the central Rad52 repair protein (Figures 2B and 7A). Furthermore, this sensitivity to DSBs was due to a profound defect in DSB repair *per se* (Figure 7C). Yra1 is an mRNA export protein, and is essential for yeast viability (60,61). Strikingly, overexpression of Yra1 leads to the accumulation of DSBs and genomic instability (62). Mechanistically, the overexpressed Yra1 and associated mRNAs re-

main on chromatin, leading to the accumulation of R-loops, which are problematic for replication forks resulting in DSB formation (62). In response to DSBs, local transcription is halted and this is required for DSB repair within transcribed genes (63). One possibility is that Yra1 is recruited to the vicinity of DSBs to export the transcripts after RNA pol II has been halted. When Yra1 levels are reduced, the resulting R loops may interfere with homologous recombinational repair of DSBs, in a similar way that the R loops block the replication machinery. However, this is unlikely to be the case, because overexpression of RNaseH1 did not reverse the DNA damage sensitivity observed upon Yra1 depletion (Supplementary Figure S7A). An alternative mechanism by which Yra1 could influence DSB repair would be a consequence of reduced export of mRNAs for key DSB repair proteins. In agreement, the human counterpart of Yra1, ALY, is required for export of Rad51 (64). However, when we examined Rad51 protein levels in the Yra1 hypomorph, they were reduced to 39–55% of the level in isogenic wild type cells (Supplementary Figure S7B). Noteworthy, there was no defect in HR repair of a single HO site at *MAT* in the *yra1* mutants (Figure 7B). This would suggest that the Rad51 levels would be sufficient for repair of a single DSB, but that the levels are insufficient to repair global DNA breaks (Figure 7C). Future studies will reveal the mechanism whereby Yra1 plays such a profound role in repair of zeocin-induced damage.

In conclusion, we have identified multiple novel histone PTMs and proteins at DSBs. Over a dozen of these proteins play novel roles in the response to DSBs. Our initial characterization of how Tom1, Sit4, Def1 and Yra1 contribute to the DNA damage response indicates that additional levels of regulation of the DNA damage response exist and remain to be delineated. Furthermore, this approach could easily be adapted to site-specific DNA breaks in mammalian cells, using the Cas9 and guide RNA components of the CRISPR system for gRNA-directed purification of a discrete section of chromatin (CRISPR-ChAP-MS) (65).

SUPPLEMENTARY DATA

Supplementary Data are available at NAR Online.

ACKNOWLEDGEMENTS

We are grateful to Virginia Zakian, Sukesh Bhaumik, Xiaolan Zhao, Weiwei Dang, Jesper Q. Svejstrup, Kevin Morano, Bing Li, Andrés Aguilera and Andreas Hochwagen for yeast strains and plasmids, and Achille Pelliccioli for the Rad53 (EL7) antibody. We are grateful to John Petrini and his lab members for use of their PFGE apparatus. We would also like to thank Bing Li for helpful discussions on Yra1, Tej Pandita for suggesting examining the effect of heat on DSB repair, and Greg Ira, Bin Wang, Nayum Kim and Xiaobing Shi for helpful suggestions. In addition, we would like to acknowledge Zih-Jie Shen, Ting-Hsiang Huang and Rhiannon Aguilar for their generous help during the paper revision. The authors would like to acknowledge the UAMS Proteomics Facility for mass spectrometric support.

FUNDING

NCI [CA95641 to J.K.T.]; NIH [R01GM106024, R21ES025268, R21DA041822, P20GM121293, UL1TR000039, P20GM103625, S10OD018445, 1P20GM121293, P20GM103429 to A.J.T.]. Funding for open access charge: Lab start up money.

Conflict of interest statement. None declared.

REFERENCES

- Mehta, A. and Haber, J.E. (2014) Sources of DNA double-strand breaks and models of recombinational DNA repair. *Cold Spring Harbor Perspect. Biol.*, **6**, a016428.
- Jackson, S.P. and Bartek, J. (2009) The DNA-damage response in human biology and disease. *Nature*, **461**, 1071–1078.
- Ciccia, A. and Elledge, S.J. (2010) The DNA damage response: making it safe to play with knives. *Mol. Cell*, **40**, 179–204.
- Chapman, J.R., Taylor, M.R. and Boulton, S.J. (2012) Playing the end game: DNA double-strand break repair pathway choice. *Mol. Cell*, **47**, 497–510.
- Tichy, E.D., Pillai, R., Deng, L., Liang, L., Tischfield, J., Schwemmer, S.J., Babcock, G.F. and Stambrook, P.J. (2010) Mouse embryonic stem cells, but not somatic cells, predominantly use homologous recombination to repair double-strand DNA breaks. *Stem Cells Dev.*, **19**, 1699–1711.
- Lok, B.H. and Powell, S.N. (2012) Molecular pathways: understanding the role of Rad52 in homologous recombination for therapeutic advancement. *Clin. Cancer Res.*, **18**, 6400–6406.
- Mazin, A.V., Mazina, O.M., Bugreev, D.V. and Rossi, M.J. (2010) Rad54, the motor of homologous recombination. *DNA Repair*, **9**, 286–302.
- Luger, K., Mader, A.W., Richmond, R.K., Sargent, D.F. and Richmond, T.J. (1997) Crystal structure of the nucleosome core particle at 2.8 Å resolution. *Nature*, **389**, 251–260.
- Rossetto, D., Truman, A.W., Kron, S.J. and Cote, J. (2010) Epigenetic modifications in double-strand break DNA damage signaling and repair. *Clin. Cancer Res.*, **16**, 4543–4552.
- Haber, J.E. (1998) Mating-type gene switching in *Saccharomyces cerevisiae*. *Annu. Rev. Genet.*, **32**, 561–599.
- Klar, A.J., Hicks, J.B. and Strathern, J.N. (1982) Directionality of yeast mating-type interconversion. *Cell*, **28**, 551–561.
- Byrum, S.D., Taverna, S.D. and Tackett, A.J. (2015) Purification of specific chromatin loci for proteomic analysis. *Methods Mol. Biol.*, **1228**, 83–92.
- Byrum, S.D., Raman, A., Taverna, S.D. and Tackett, A.J. (2012) ChAP-MS: a method for identification of proteins and histone posttranslational modifications at a single genomic locus. *Cell Rep.*, **2**, 198–205.
- Longtine, M.S., McKenzie, A. 3rd, Demarini, D.J., Shah, N.G., Wach, A., Brachat, A., Philippsen, P. and Pringle, J.R. (1998) Additional modules for versatile and economical PCR-based gene deletion and modification in *Saccharomyces cerevisiae*. *Yeast*, **14**, 953–961.
- Sandell, L.L. and Zakian, V.A. (1993) Loss of a yeast telomere: arrest, recovery, and chromosome loss. *Cell*, **75**, 729–739.
- Chaurasia, P., Sen, R., Pandita, T.K. and Bhaumik, S.R. (2012) Preferential repair of DNA double-strand break at the active gene in vivo. *J. Biol. Chem.*, **287**, 36414–36422.
- Keogh, M.C., Kim, J.A., Downey, M., Fillingham, J., Chowdhury, D., Harrison, J.C., Onishi, M., Datta, N., Galicia, S., Emili, A. et al. (2006) A phosphatase complex that dephosphorylates gammaH2AX regulates DNA damage checkpoint recovery. *Nature*, **439**, 497–501.
- Fiorani, S., Mimun, G., Caleca, L., Piccini, D. and Pelliccioli, A. (2008) Characterization of the activation domain of the Rad53 checkpoint kinase. *Cell Cycle*, **7**, 493–499.
- Tamburini, B.A. and Tyler, J.K. (2005) Localized histone acetylation and deacetylation triggered by the homologous recombination pathway of double-strand DNA repair. *Mol. Cell Biol.*, **25**, 4903–4913.
- Byrum, S.D., Taverna, S.D. and Tackett, A.J. (2013) Purification of a specific native genomic locus for proteomic analysis. *Nucleic Acids Res.*, **41**, e195.
- Herskowitz, I. and Jensen, R.E. (1991) Putting the HO gene to work: practical uses for mating-type switching. *Methods Enzymol.*, **194**, 132–146.
- White, C.I. and Haber, J.E. (1990) Intermediates of recombination during mating type switching in *Saccharomyces cerevisiae*. *EMBO J.*, **9**, 663–673.
- Chen, C.C., Carson, J.J., Feser, J., Tamburini, B., Zaboronick, S., Linger, J. and Tyler, J.K. (2008) Acetylated lysine 56 on histone H3 drives chromatin assembly after repair and signals for the completion of repair. *Cell*, **134**, 231–243.
- Maas, N.L., Miller, K.M., DeFazio, L.G. and Toczyski, D.P. (2006) Cell cycle and checkpoint regulation of histone H3 K56 acetylation by Hst3 and Hst4. *Mol. Cell*, **23**, 109–119.
- Masumoto, H., Hawke, D., Kobayashi, R. and Verreault, A. (2005) A role for cell-cycle-regulated histone H3 lysine 56 acetylation in the DNA damage response. *Nature*, **436**, 294–298.
- Robzyk, K., Recht, J. and Osley, M.A. (2000) Rad6-dependent ubiquitination of histone H2B in yeast. *Science*, **287**, 501–504.
- Schuldiner, M., Collins, S.R., Thompson, N.J., Denic, V., Bhamidipati, A., Punna, T., Ihmels, J., Andrews, B., Boone, C., Greenblatt, J.F. et al. (2005) Exploration of the function and organization of the yeast early secretory pathway through an epistatic miniarray profile. *Cell*, **123**, 507–519.
- Kampinga, H.H. and Konings, A.W. (1987) Inhibition of repair of X-ray-induced DNA damage by heat: the role of hyperthermic inhibition of DNA polymerase alpha activity. *Radiat. Res.*, **112**, 86–98.
- Hunt, C.R., Pandita, R.K., Laszlo, A., Higashikubo, R., Agarwal, M., Kitamura, T., Gupta, A., Rief, N., Horikoshi, N., Baskaran, R. et al. (2007) Hyperthermia activates a subset of ataxia-telangiectasia mutated effectors independent of DNA strand breaks and heat shock protein 70 status. *Cancer Res.*, **67**, 3010–3017.
- Pandita, T.K., Pandita, S. and Bhaumik, S.R. (2009) Molecular parameters of hyperthermia for radiosensitization. *Crit. Rev. Eukaryotic Gene Express.*, **19**, 235–251.
- Hunt, C.R., Dix, D.J., Sharma, G.G., Pandita, R.K., Gupta, A., Funk, M. and Pandita, T.K. (2004) Genomic instability and enhanced radiosensitivity in Hsp70.1- and Hsp70.3-deficient mice. *Mol. Cell Biol.*, **24**, 899–911.
- Ray, B.L., White, C.I. and Haber, J.E. (1991) Heteroduplex formation and mismatch repair of the “stuck” mutation during mating-type switching in *Saccharomyces cerevisiae*. *Mol. Cell Biol.*, **11**, 5372–5380.
- Saleh, A., Collart, M., Martens, J.A., Genereaux, J., Allard, S., Cote, J. and Brandl, C.J. (1998) TOM1p, a yeast hctt-domain protein which mediates transcriptional regulation through the ADA/SAGA coactivator complexes. *J. Mol. Biol.*, **282**, 933–946.
- Singh, R.K., Kabbaj, M.H., Paik, J. and Gunjan, A. (2009) Histone levels are regulated by phosphorylation and ubiquitylation-dependent proteolysis. *Nat. Cell Biol.*, **11**, 925–933.
- Lazzaro, F., Giannattasio, M., Puddu, F., Granata, M., Pelliccioli, A., Plevani, P. and Muzi-Falconi, M. (2009) Checkpoint mechanisms at the intersection between DNA damage and repair. *DNA Repair (Amst.)*, **8**, 1055–1067.
- Vaze, M.B., Pelliccioli, A., Lee, S.E., Ira, G., Liberi, G., Arbel-Eden, A., Foiani, M. and Haber, J.E. (2002) Recovery from checkpoint-mediated arrest after repair of a double-strand break requires Srs2 helicase. *Mol. Cell*, **10**, 373–385.
- Pelliccioli, A., Lee, S.E., Lucca, C., Foiani, M. and Haber, J.E. (2001) Regulation of *Saccharomyces* Rad53 checkpoint kinase during adaptation from DNA damage-induced G2/M arrest. *Mol. Cell*, **7**, 293–300.
- Stefansson, B. and Brautigan, D.L. (2006) Protein phosphatase 6 subunit with conserved Sit4-associated protein domain targets IkkappaBepsilon. *J. Biol. Chem.*, **281**, 22624–22634.
- Sutton, A., Immanuel, D. and Arndt, K.T. (1991) The SIT4 protein phosphatase functions in late G1 for progression into S phase. *Mol. Cell Biol.*, **11**, 2133–2148.
- Woudstra, E.C., Gilbert, C., Fellows, J., Jansen, L., Brouwer, J., Erdjument-Bromage, H., Tempst, P. and Svejstrup, J.Q. (2002) A Rad26-Def1 complex coordinates repair and RNA pol II proteolysis in response to DNA damage. *Nature*, **415**, 929–933.

41. Jha, D.K. and Strahl, B.D. (2014) An RNA polymerase II-coupled function for histone H3K36 methylation in checkpoint activation and DSB repair. *Nat. Commun.*, **5**, 3965.
42. Strasser, K. and Hurt, E. (2000) Yra1p, a conserved nuclear RNA-binding protein, interacts directly with Mex67p and is required for mRNA export. *EMBO J.*, **19**, 410–420.
43. Haruki, H., Nishikawa, J. and Laemmli, U.K. (2008) The anchor-away technique: rapid, conditional establishment of yeast mutant phenotypes. *Mol. Cell.*, **31**, 925–932.
44. Shroff, R., Arbel-Eden, A., Pilch, D., Ira, G., Bonner, W.M., Petrini, J.H., Haber, J.E. and Lichten, M. (2004) Distribution and dynamics of chromatin modification induced by a defined DNA double-strand break. *Curr. Biol.*, **14**, 1703–1711.
45. Han, J., Zhang, H., Zhang, H., Wang, Z., Zhou, H. and Zhang, Z. (2013) A Cul4 E3 ubiquitin ligase regulates histone hand-off during nucleosome assembly. *Cell*, **155**, 817–829.
46. Cagney, G., Alvaro, D., Reid, R.J., Thorpe, P.H., Rothstein, R. and Krogan, N.J. (2006) Functional genomics of the yeast DNA-damage response. *Genome Biol.*, **7**, 233.
47. Ben-Shitrit, T., Yosef, N., Shemesh, K., Sharan, R., Rupp, E. and Kupiec, M. (2012) Systematic identification of gene annotation errors in the widely used yeast mutation collections. *Nat. Methods*, **9**, 373–378.
48. Giaever, G., Chu, A.M., Ni, L., Connelly, C., Riles, L., Veronneau, S., Dow, S., Lucau-Danila, A., Anderson, K., Andre, B. *et al.* (2002) Functional profiling of the *Saccharomyces cerevisiae* genome. *Nature*, **418**, 387–391.
49. Yuen, K.W., Warren, C.D., Chen, O., Kwok, T., Hieter, P. and Spencer, F.A. (2007) Systematic genome instability screens in yeast and their potential relevance to cancer. *Proc. Natl. Acad. Sci. U.S.A.*, **104**, 3925–3930.
50. Franken, N.A. and Barendsen, G.W. (2014) Enhancement of radiation effectiveness by hyperthermia and incorporation of halogenated pyrimidines at low radiation doses as compared with high doses: implications for mechanisms. *Int. J. Radiat. Biol.*, **90**, 313–317.
51. Bergs, J.W., Franken, N.A., Haveman, J., Geijsen, E.D., Crezee, J. and van Bree, C. (2007) Hyperthermia, cisplatin and radiation trimodality treatment: a promising cancer treatment? A review from preclinical studies to clinical application. *Int. J. Hyperthermia*, **23**, 329–341.
52. Bastians, H. and Ponstingl, H. (1996) The novel human protein serine/threonine phosphatase 6 is a functional homologue of budding yeast Sit4p and fission yeast ppe1, which are involved in cell cycle regulation. *J. Cell Sci.*, **109**, 2865–2874.
53. Douglas, P., Zhong, J., Ye, R., Moorhead, G.B., Xu, X. and Lees-Miller, S.P. (2010) Protein phosphatase 6 interacts with the DNA-dependent protein kinase catalytic subunit and dephosphorylates gamma-H2AX. *Mol. Cell Biol.*, **30**, 1368–1381.
54. Soriano-Carot, M., Quilis, I., Bano, M.C. and Igual, J.C. (2014) Protein kinase C controls activation of the DNA integrity checkpoint. *Nucleic Acids Res.*, **42**, 7084–7095.
55. Angeles de la Torre-Ruiz, M., Torres, J., Arino, J. and Herrero, E. (2002) Sit4 is required for proper modulation of the biological functions mediated by Pkc1 and the cell integrity pathway in *Saccharomyces cerevisiae*. *J. Biol. Chem.*, **277**, 33468–33476.
56. Hauer, M.H., Seeber, A., Singh, V., Thierry, R., Sack, R., Amitai, A., Kryzhanovska, M., Eglinger, J., Holcman, D., Owen-Hughes, T. *et al.* (2017) Histone degradation in response to DNA damage enhances chromatin dynamics and recombination rates. *Nat. Struct. Mol. Biol.*, **24**, 99–107.
57. Daraba, A., Gali, V.K., Halmi, M., Haracska, L. and Unk, I. (2014) Def1 promotes the degradation of Pol3 for polymerase exchange to occur during DNA-damage-induced mutagenesis in *Saccharomyces cerevisiae*. *PLoS Biol.*, **12**, e1001771.
58. Chen, Y.B., Yang, C.P., Li, R.X., Zeng, R. and Zhou, J.Q. (2005) Def1p is involved in telomere maintenance in budding yeast. *J. Biol. Chem.*, **280**, 24784–24791.
59. Jordan, P.W., Klein, F. and Leach, D.R. (2007) Novel roles for selected genes in meiotic DNA processing. *PLoS Genet.*, **3**, e222.
60. Preker, P.J., Kim, K.S. and Guthrie, C. (2002) Expression of the essential mRNA export factor Yra1p is autoregulated by a splicing-dependent mechanism. *RNA*, **8**, 969–980.
61. Portman, D.S., O'Connor, J.P. and Dreyfuss, G. (1997) YRA1, an essential *Saccharomyces cerevisiae* gene, encodes a novel nuclear protein with RNA annealing activity. *RNA*, **3**, 527–537.
62. Gavalda, S., Santos-Pereira, J.M., Garcia-Rubio, M.L., Luna, R. and Aguilera, A. (2016) Excess of Yra1 RNA-binding factor causes transcription-dependent genome instability, replication impairment and telomere shortening. *PLoS Genet.*, **12**, e1005966.
63. Pankotai, T. and Soutoglou, E. (2013) Double strand breaks: hurdles for RNA polymerase II transcription? *Transcription*, **4**, 34–38.
64. Wickramasinghe, V.O., Savill, J.M., Chavali, S., Jonsdottir, A.B., Rajendra, E., Gruner, T., Laskey, R.A., Babu, M.M. and Venkitaraman, A.R. (2013) Human inositol polyphosphate multikinase regulates transcript-selective nuclear mRNA export to preserve genome integrity. *Mol. Cell*, **51**, 737–750.
65. Waldrip, Z.J., Byrum, S.D., Storey, A.J., Gao, J., Byrd, A.K., Mackintosh, S.G., Wahls, W.P., Taverna, S.D., Raney, K.D. and Tackett, A.J. (2014) A CRISPR-based approach for proteomic analysis of a single genomic locus. *Epigenetics*, **9**, 1207–1211.